Case Study

New cycloid rotor profiles design under different rolling circle radii for Roots vacuum pumps

Zhengqing Li[1] · Xiaojun Wang[1]

Received: 9 May 2022 / Accepted: 21 September 2022
Published online: 30 September 2022

Abstract
This study presents two new cycloid rotor profiles for Roots vacuum pump formed by different rolling circle radii to improve the volume utilization rate and compression ratio. A new rotor profile composed of a pin-tooth arc and a cycloid is design and analyzed where its rolling circle radius is larger than 1/4 of the pitch radius. As the rolling circle radius increases, the volume utilization rate continues to increase and can be greater than 60%, which is an increase of 20% relative to the standard cycloid profile. In addition, another new rotor profile composed of a large arc and a cycloid is designed and analyzed where its rolling circle radius is smaller than 1/4 of the pitch radius. As the rolling circle radius decreases, the length of the minimum gap between rotor profile and chamber increases, which is beneficial for improving the compression ratio and reducing backflow.

Article highlights

1. Two new rotor profiles are proposed and designed to improve the performance for Roots vacuum pump.
2. For the new rotor profile formed by a large rolling circle, its volume utilization rate is greater than 60%, which can pump more gas in a cycle and significantly better than that of traditional profile, such as arc profile.
3. For the new rotor profile formed by a small rolling circle, its pressure ratio is greater than traditional rotor profiles because its length of minimum gap between rotor profile and chamber is critical increased to decrease the back flow.

Keywords Roots vacuum pump · Cycloid · Conjugate · Rotor · Profile · Rolling circle

1 Introduction

A Roots vacuum pump is a double-rotor rotary and volumetric pump. During its operation, the two rotors rotate toward each other to transport gas from the inlet to the outlet to pump the gas. Owing to their fast start-up, low power consumption, high pumping speed, high efficiency, and low maintenance costs, Roots vacuum pumps are widely used in the semiconductor, metallurgy, chemical, pharmaceutical, and other industries. The rotors mesh with each other during the operation to reduce backflow. Therefore, the mesh design of the rotor profile of Roots vacuum pumps is important. Several studies have been conducted on the analysis of rotor profiles and the

✉ Zhengqing Li, ahanda-nwpu@163.com | [1]Lanzhou Institute of Physics, China Academy of Space, Lanzhou 730000, China.

exploration of new rotor profiles based on meshing characteristics, which are directly related to the performance indicators of the pump [1, 2].

Traditional rotor profiles for Roots vacuum pumps are applied in several pumps and mainly divided into three types: cycloid, involute, and arc [3–5]. Meanwhile, new types of rotor profiles have been explored to improve the performance of Roots vacuum pumps. An elliptical rotor profile having three independent geometric parameters and a relatively higher area efficiency compared with the traditional rotor profile was studied [6]. An involute and variable extend cycloid profile for multiple stages was proposed, and a Roots vacuum pump was designed to obtain a better geometric performance than traditional rotor profiles [7]. A fifth-order polynomial and cubic spline were employed to produce a trochoidal rotor profile with a variable trochoid ratio to generate a smooth trochoid motion function [8]. To improve the design efficiency of the profile, an integrated automated system for rotor design was developed to obtain a theoretical profile for an internal lobe pump, where the outer rotor is typically characterized by lobes with an elliptical shape, and the inner rotor profile is a conjugate curve [9]. Based on the principles of instantaneous center and homogeneous coordinate transformation, a geometric approach was proposed to study rotor profiles that consist of two circular arcs [10]. To provide an efficient and intuitive approach for design, analysis, and development, Roots rotor tooth profiles were generated using arc-cycloidal curves and arc-involute curves via an Assur-group-associated virtual linkage method [11]. In addition, the performance parameters of the Roots vacuum pump were studied to select the optimal rotor profiles using Ansys and Fluent software programs. A three-dimensional numerical approach was developed using computational fluid dynamics. The fluid analysis models of cylindrical- and screw-type Roots vacuum pumps revealed the differences in their flow characteristics and demonstrated their better average outlet flow rates; they also showed that the cylindrical-type pump is better than the screw-type one [12, 13].

These studies explore new rotor profiles to increase the volume utilization and enhance the performance parameters, such as pressure ratio, effective pumping speed, and ultimate vacuum. The rolling circle radius of the standard cycloid rotor profile is 1/4 of the pitch radius, and the volume utilization rate is 50%. Compared with the arc and involute rotor profiles, the standard cycloid profile has only one independent variable, which limits its applications [14].

In next section, a new rotor profile composed of a cycloid and a pin-tooth arc is designed where the rolling circle radius is larger than 1/4 of the pitch radius; and another new rotor profile composed of a cycloid and a large arc is designed where the rolling circle radius is smaller than 1/4 of the pitch radius. Section 3 shows the volume utilization rate of the rotor profile obtained by the large rolling circle increases and can exceed 60% as the rolling circle increases which can pump more gas, and the length of minimum gap between rotor profile and chamber is critical increased as the rolling circle radius decreases for the rotor profile obtained by the small rolling circle radius which can improve its compression ratio and decrease the back flow. In Sect. 4, a summary and conclusion of results are given.

2 Rotor profile analysis

The rotor profile of a Roots vacuum pump is centrosymmetric and axisymmetric. One-fourth of the entire rotor profile must be designed. As shown in Figs. 1 and 2, b is the rolling circle radius and R_1 is the pitch circle radius. When the profile is the standard cycloid rotor profile, $b = R_1/4$, and the curve AC is the epicycloid. In Fig. 1, the rolling circle radius is larger than the standard $b > R_1/4$, which corresponds to a cycloid with a large rolling circle. When the rolling circle rolls to point F at the top of the pitch circle, point A on the circle rolls to point E. The curve AE is an epicycloid, and the curve CE can be used to design a pin-tooth arc, where the arc center is point F and the arc radius is R_2 = EF. For the meshing characteristics, the waist curve AB is the conjugate curve of AC. In Fig. 2, the rolling circle radius is smaller than the standard $b < R_1/4$, which corresponds to a cycloid with a small rolling circle. When the rolling circle passes an angle π, point A reaches point E. The curve AE is an epicycloid, and the CE curve is designed as a large arc, where the center of the arc is point O and the

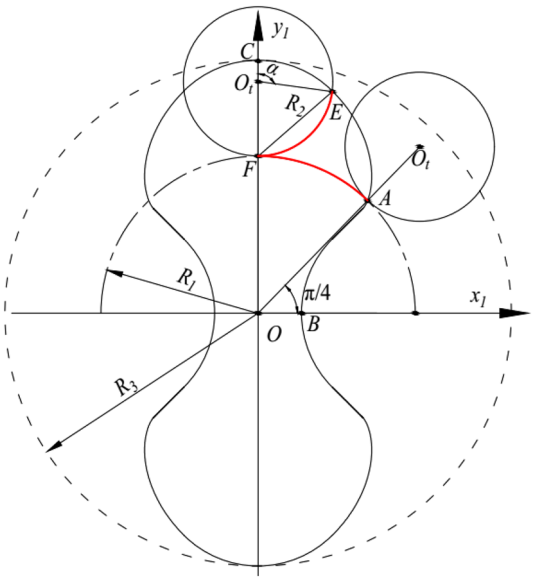

Fig. 1 Profile with a large rolling circle

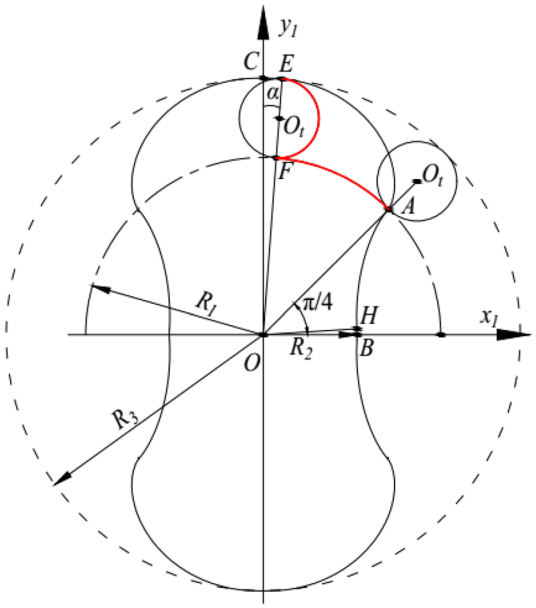

Fig. 2 Profile with a small rolling circle

radius of the arc is $R_3 = \mathrm{OE} = R_1 + 2b$. For the meshing characteristics, the waist curve AB is the conjugate curve of AC.

2.1 Cycloid profile with a large rolling circle

In Fig. 1, the rolling circle is tangent to the pitch circle at point A at the initial moment. When the rolling circle rolls from point A to point E, the curve formed is the epicycloid of the rotor profile. The arc length EF is $(\pi - \alpha)b$, and the arc length AF corresponding to the pitch circle is $\pi R_1/4$. Regarding the characteristics of the cycloid, the two arc lengths are equal and can be expressed as

$$\alpha = \pi - \frac{\pi R_1}{4b}. \tag{1}$$

The arc CE is a pin-tooth arc with point F as the center and EF as the radius. The length of EF can be expressed as

$$R_2 = 2b\cos\frac{\alpha}{2}. \tag{2}$$

Therefore, the curve AC is composed of two parts: an epicycloid AE and a pin-tooth arc line CE for a cycloid profile with a large rolling circle.

When the rolling circle rolls from the initial point A to any point A′, as shown in Fig. 3, the central angle of the rolling circle is γ, the angle between OO_t and OA is θ, O_tM is parallel to Ox_1, and the angle between O_tM and OA′ is β. β can be expressed as [4]

$$\beta = \theta + \gamma - \frac{3\pi}{4}. \tag{3}$$

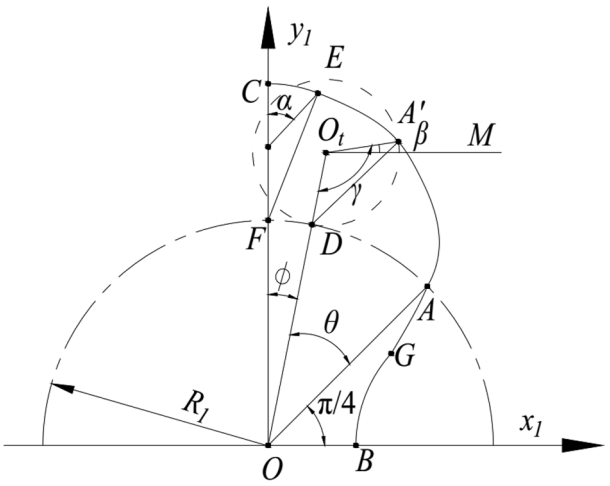

Fig. 3 Analysis of a cycloid rotor profile with a large rolling circle

The arc length rolled by the rolling circle is $\mathrm{DA}' = b\gamma$ and the arc length of the pitch circle passed by the rolling circle is $\mathrm{DA} = \theta R_1$. They are equal and can be expressed as follows:

$$\gamma = \frac{R_1}{b}\theta. \tag{4}$$

In $\Delta O_tOA'$, $\boldsymbol{OA'}$ can be expressed as

$$\boldsymbol{OA'} = \boldsymbol{OO_t} + \boldsymbol{O_tA'}, \tag{5}$$

where $\boldsymbol{OA}$ is (x_1, y_1), $\boldsymbol{O_tO}$ is $\left(\left(R_1 + b\right)\cos(\theta + \pi/4), \left(R_1 + b\right)\sin(\theta + \pi/4)\right)$, and $\boldsymbol{O_tA'}$ is $(b\cos\beta, b\sin\beta)$. Therefore, combining Eqs. (3)–(5), $\boldsymbol{OA}$ can be expressed as

$$\begin{cases} x_1 = \left(R_1 + b\right)\cos\left(\theta + \frac{\pi}{4}\right) - b\cos\left(\frac{R_1+b}{b}\theta + \frac{\pi}{4}\right) \\ y_1 = \left(R_1 + b\right)\sin\left(\theta + \frac{\pi}{4}\right) - b\sin\left(\frac{R_1+b}{b}\theta + \frac{\pi}{4}\right) \end{cases}. \tag{6}$$

The range of θ corresponding to the epicycloid AE of the rotor is $(0, \pi/4)$ in Eq. (6).

The top pin-tooth arc CE can be expressed as

$$\begin{cases} x_1 = R_2\cos\left(\frac{\pi}{2} - \varphi\right) \\ y_1 = R_1 + R_2\sin\left(\frac{\pi}{2} - \varphi\right) \end{cases}. \tag{7}$$

The range of φ is $(0, \alpha/2)$ in Eq. (7).

The top and waist curves of the two rotors of the Roots vacuum pump mesh together during its operation. When using the meshing characteristics to obtain the profile corresponding to the conjugate curve of the rotor, the meshing angle ϕ of the rotor, that is, the angle between the line

O_tO and coordinate Oy_1, must be obtained. Therefore, in the epicycloid AE, $\phi = \pi/4 - \theta$ and its range is $(0, \pi/4)$.

Regarding the meshing characteristics, the top arc CE corresponding to the waist meshing curve is the pin-tooth arc GB and can be expressed as

$$\begin{cases} x_1 = R_1 + R_2 \cos(\pi - \varphi) \\ y_1 = R_2 \sin(\pi - \varphi) \end{cases}. \tag{8}$$

The range of φ is $(0, \alpha/2)$ in Eq. (8).

2.2 Cycloid profile with a small rolling circle

As shown in Fig. 2, when the rolling circle rolls from point A to point E, the formed curve AE is the epicycloid of the rotor profile. The arc length of the rolling circle is πb, and the arc length corresponding to the pitch circle is $(\pi/4 - \alpha)R_1$. Regarding the characteristics of the cycloid, the two curves are equal and can be expressed as

$$\alpha = \frac{\pi}{4} - \frac{b\pi}{R_1}. \tag{9}$$

The arc CE is a large arc with point O as the center and OE as the radius. Then, the length of OE can be expressed as

$$R_3 = R_1 + 2b. \tag{10}$$

Therefore, the curve AC is composed of two parts: an epicycloid AE and a large arc CE for a cycloid profile with a small rolling circle.

In Fig. 4, when the rolling circle rolls from the initial point A to any point A′, the central angle of the rolling circle is γ, the angle between OO_t and OA is θ, O_tM is parallel to Ox_1, and the angle between O_tM and OA′ is β, which is determined using Eq. (3).

The epicycloid AE of the rotor is determined using Eq. (6), and the range of θ is $(0, \pi/4 - \alpha)$. The large arc CE can be expressed as

$$\begin{cases} x_1 = (R_1 + 2b)\cos\theta \\ y_1 = (R_1 + 2b)\sin\theta \end{cases}. \tag{11}$$

The range of θ is $(\pi/2 - \alpha, \pi/2)$ in Eq. (11). As CE is a large arc, the gap between this arc and the chamber of the Roots vacuum pump is maintained at a constant value, which is different from other rotor profile lines, in which only a minimum gap is formed between the top point and the chamber. The large arc of the rotor profile with a small rolling circle evidently reduces the backflow of gas, which is of considerable significance for improving the compression ratio and ultimate vacuum.

The meshing angle of the small rolling circle is $\phi = \pi/4 - \theta$ and its range is $(\alpha, \pi/4)$; for the arc CE,

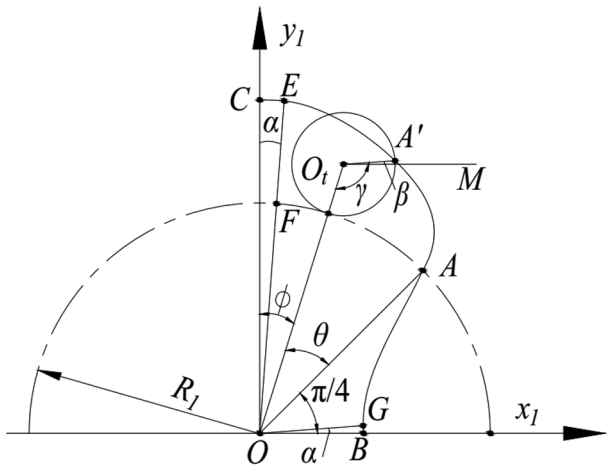

Fig. 4 Analysis of a cycloid rotor profile with a small rolling circle

according to the meshing characteristics, its meshing curve GB is the arc with the center O, and the arc radius is $R_2 = R_1 - 2b$. Therefore, its equation can be expressed as

$$\begin{cases} x_1 = (R_1 - 2b)\cos\varphi \\ y_1 = (R_1 - 2b)\sin\varphi \end{cases}. \tag{12}$$

The range of φ is $(0, \alpha)$ in Eq. (12).

2.3 Conjugate curve

A conjugate curve can be defined as a pair of smooth curves with a given law of motion that maintain continuous tangential contact according to a given contact method during the movement [11].

As shown in Fig. 5, two coordinate systems were fixed to the rotors. According to the coordinate conversion relationship, the conversion relationship between coordinate systems S1 and S2 is expressed as [10]

$$\begin{cases} x_2 = x_1 \cos 2\phi - y_1 \sin 2\phi + 2R_1 \sin\phi \\ y_2 = x_1 \sin 2\phi + y_1 \cos 2\phi - 2R_1 \cos\phi \end{cases}. \tag{13}$$

The conjugate curve A′C′ was obtained by solving Eq. (13) in the S2 coordinate system meshing to the curve AC in the S1 coordinate system, where (x_1, y_1) is determined using Eq. (6). Based on the characteristics of the rotor profile, the conjugate curve A′C′ in the S2 coordinate system has exactly the same shape as the rotor part AB in the S1 coordinate system. This curve must be translated to S1 and rotated counterclockwise to obtain AB using Eq. (14).

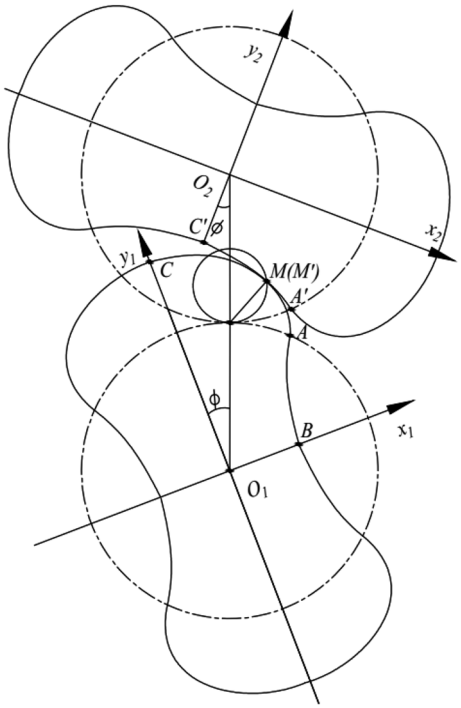

Fig. 5 Transformation of the coordinate system in the conjugate curve

$$\begin{cases} x_1' = -\left(x_1 \sin 2\phi + y_1 \cos 2\phi - 2R_1 \cos\phi\right) \\ y_1' = x_1 \cos 2\phi - y_1 \sin 2\phi + 2R_1 \sin\phi \end{cases} \quad (14)$$

Therefore, AB and AC form the cycloid of the rotor profile, and the entire rotor profile is obtained according to the symmetry of AB and AC.

Based on Eq. (14), the conjugate curve AG is obtained for the cycloid profiles with a large rolling circle and a small rolling circle, as shown in Figs. 3 and 4.

3 Cycloid rotor profile design

According to the above analysis, the rotor profile of the Roots vacuum pump was designed, where the actual pumping speed was 70 L/s, the rotating speed was 3000 r/min, the effective pumping speed was 75%, and the rotor pitch radius was $R_1 = 34$ mm.

3.1 Cycloid rotor profile design with a large rolling circle

In the design of the cycloid rotor profile with a large rolling circle, when the ratio of the pitch circle radius to the rolling circle radius $c = R_1/b$ is 4.0, 3.5, 3.0, 2.5, 2.0, 1.5, and 1.0, the radius of the rotor pin-tooth arc R_1, the radius of the pin-tooth circle R_2, the radius of the top circle R_3, the volume utilization rate λ, and length l of the rotor profile are analyzed and calculated.

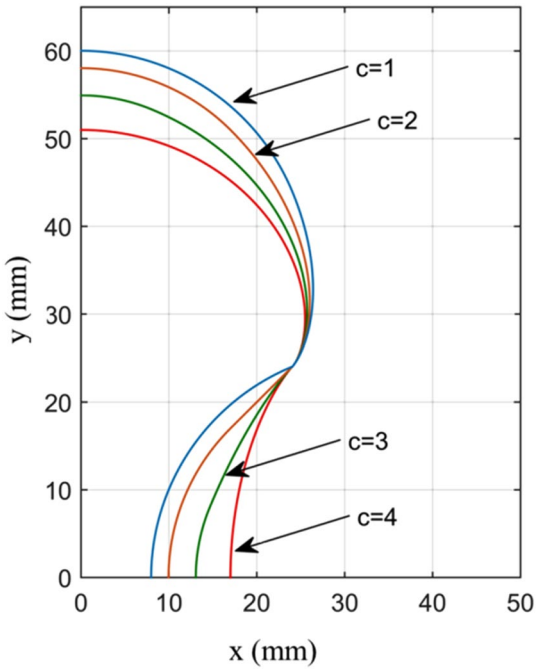

Fig. 6 1/4 Rotor profile

The epicycloid AE of the 1/4 rotor profile is expressed as

$$\begin{cases} x_1 = \left(R_1 + b\right)\cos\left(\theta + \frac{\pi}{4}\right) - b\cos\left[(c+1)\theta + \frac{\pi}{4}\right] \\ y_1 = \left(R_1 + b\right)\sin\left(\theta + \frac{\pi}{4}\right) - b\sin\left[(c+1)\theta + \frac{\pi}{4}\right] \end{cases}. \quad (15)$$

The range of θ corresponding to the epicycloid AE of the rotor is $(0, \pi/4)$ in Eq. (15).

As shown in Fig. 3, the top pin-tooth arc is determined using Eq. (7), the conjugate curve AG corresponding to the epicycloid AE can be determined using Eq. (14), and the arc of the waist pin tooth is determined using Eq. (8). First, 1/4 rotor profiles were obtained for different values of c, as shown in Fig. 6. Then, a 1/4 rotor profile was constructed symmetrically to obtain the entire theoretical profile of the rotor, as shown in Fig. 7. The parameters used are listed in Table 1.

In Fig. 7, as c decreases, the waist of the rotor profile becomes thinner and the top becomes higher. Therefore, if c is small, R_2 is large. In Table 1, as c decreases, R_2 and α increase, this indicates that the length of the pin-tooth arc and volume utilization rate also increase. Therefore, the length l of the rotor decreases at the same pumping speed. In particular, when $c = 4$, the profile is a standard cycloid, and when $c = 1$, the radius of the rolling circle is equal to the radius of the pitch circle corresponding to

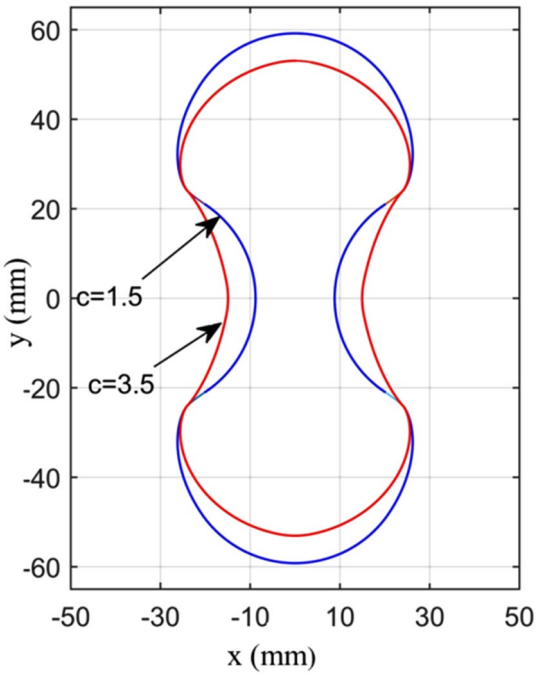

Fig. 7 Rotor profile

the maximum rolling circle. Furthermore, when $c \leq 2$, the volume utilization rate is $\lambda \geq 0.5945$, which is significantly better than that of the arc and involute rotor profiles and 20% better than that of the standard cycloid profile. In real product design, c can be selected as 2.0. The length of the rotor is then rounded to 150 mm.

3.2 Cycloid rotor profile design with a small rolling circle

According to the design of the cycloid rotor profile with a small rolling circle, when the ratios of the pitch circle radius to the rolling circle radius $c = R_1/b$ are 4.00, 4.05, 4.10, 4.15, and 4.20, the radius of the large arc R_3, the volume utilization coefficient λ, and the length l of the rotor are analyzed and calculated.

The epicycloid AE of the 1/4 rotor profile is determined using Eq. (15), and the range of θ is $(0, \pi/4 - \alpha)$. The large arc CE is determined using Eq. (11), the conjugate curve AG corresponding to the epicycloid AE is determined using Eq. (14), and the waist arc GB is determined using Eq. (12). The rotor profile is shown in Fig. 8. The top circle radius R_3, volume utilization rate λ, and rotor length l are listed in Table 2.

In Fig. 8, the red arc is a large arc, and its central angle is defined as $\Psi = 2\alpha$. For the angle Ψ of the top rotor profile, the gap between the rotor and the chamber of the Roots vacuum pump is minimum and constant. As shown in Table 2 and Fig. 9, as c increases, R_3 decreases, but Ψ increases, indicating that the length of the large arc increases, although the volume utilization rate decreases. When $c = 4$, the rotor profile is a standard cycloid and the length of the large arc is zero. Compared with the standard cycloid rotor profile, the volume utilization rate was reduced for the rotor profile with a small rolling circle, but the decrease was very small. For example, for $c = 4.20$, the volume utilization rate was only 2.24% lower than that of the standard cycloid rotor profile. In addition, as shown in Fig. 8, the length of the minimum gap between the rotor and the chamber increases, as c increases, and the flow conductance for a gas can be estimated using Eq. (16).

$$C = \eta \bar{v} \frac{l^3}{R_3 \psi} \tag{16}$$

where C is the flow conductance, η is a constant, and $\bar{v}$ is the average speed of the gas. As ψ increases, the flow conductance decreases, which indicates that the backflow rate decreases. This is useful for improving the ultimate vacuum, compression ratio, and pumping speed. Therefore, $c = 4.20$ can be selected, and the rotor length is rounded to 245 mm on the theoretical length of rotor $l = 241.26$ mm.

3.3 Discussion

Volume utilization rate and minimum gap are core parameters of rotor profile design. For the volume utilization rate of common rotor profiles, the arc rotor profile is not more than 58%, the involute rotor profile is not more than 60%, and the standard cycloid rotor profile is 50% [13, 15]. However, the cycloid rotor profile designed with a large rolling circle is greater than 60% in volume utilization rate. Therefore, it has the advantage in volume utilization

Table 1 Parameters of the rotor profile with a large rolling circle for different values of c

R_1 (mm)	34	34	34	34	34	34	34
c	4.0	3.5	3.0	2.5	2.0	1.5	1.0
α (°)	0	22.5	45	67.5	90	112.5	135
R_2 (mm)	17.04	19.06	20.94	22.62	24.04	25.19	26.06
R_3 (mm)	51.04	53.06	54.94	56.62	58.04	59.19	60.06
λ	0.5	0.532	0.5575	0.5787	0.5945	0.6074	0.6152
l (mm)	228.2	198.4	176.55	160.16	148.33	139.63	134.05

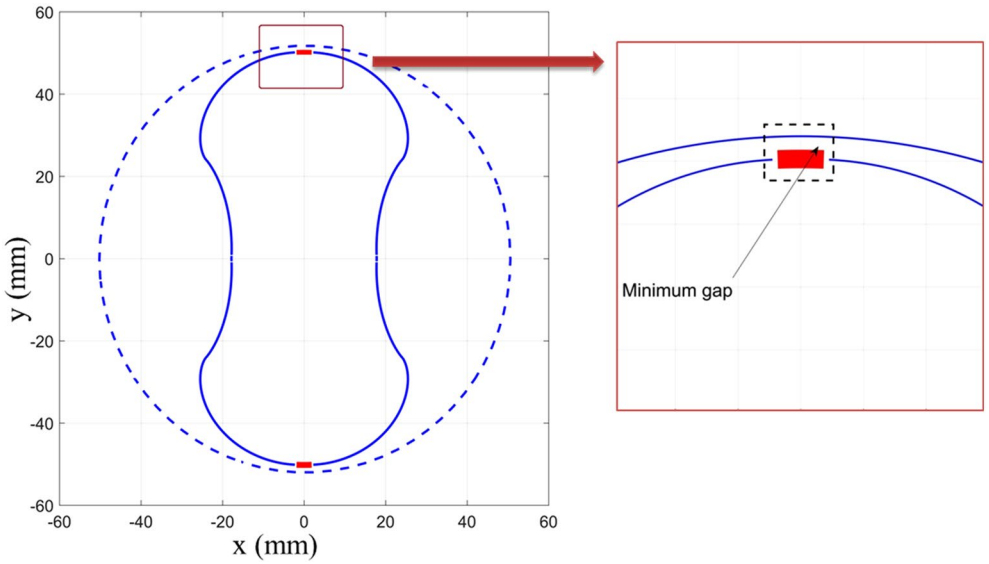

Fig. 8 Cycloid rotor profile with a small rolling circle

Table 2 Parameters of the rotor profile with a small rolling circle for different values of *c*

R_1 (mm)	34	34	34	34	34
c	4.0	4.05	4.10	4.15	4.20
α (°)	0	1.75	3.45	5.11	6.73
R_3 (mm)	51.04	50.79	50.59	50.39	50.19
λ	0.5	0.4976	0.4945	0.4916	0.4888
l (mm)	228.2	231.46	234.78	238.05	241.26

rate obviously which means the Roots vacuum pump can pump more gas than other rotor profiles. On the other hand, for the minimum gap between rotor and chamber, it is just a point for the arc rotor profile, the involute rotor profile and the standard cycloid rotor profile, but it is a part of arc for the cycloid rotor profile designed with a small rolling circle. The flow resistance of minimum gap is proportional to the length of the minimum gap, but the backflow rate through the minimum gap is inversely proportional to the length of the minimum gap which means

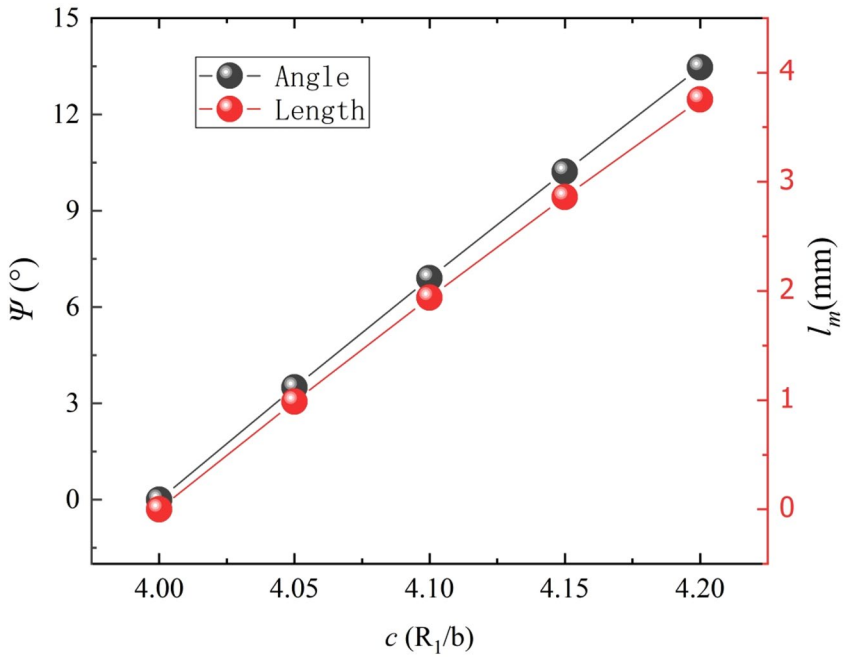

Fig. 9 Angle and length of the minimum gap for different values of *c*, $l_m = R_3\Psi$ is the length of the large arc

the backflow rate is inversely proportional to the length of minimum gap. Therefore, the effective pumping speed and compression ratio can be significantly improved for the cycloid rotor profile designed with a small rolling circle compared with common profiles, which is inversely proportional to backflow rate. Obviously, the cycloid rotor profile designed with a small rolling circle has advantage in the effective pumping speed and compression rate. Finally, whether the new cycloid profile formed by a large or small rolling circle, the volume utilization rate and the minimum gap length are not optimized simultaneous. Therefore, further research to explore new profiles is necessary to improve both volume utilization rate and minimum gap length.

4 Conclusions

The design of the cycloid rotor profile mainly determines the pitch circle radius and the radius ratio of the rolling circle to the pitch circle; thus, the design of the cycloid rotor profile has two independent variables. The meshing characteristics are used to obtain a hypocycloid in the design of the conjugate curve. In the design of a cycloid rotor profile with a large rolling circle, the rolling circle radius is greater than 1/4 of the pitch circle radius, which yields a new cycloid rotor profile composed of an epicycloid, a hypocycloid, and pin-tooth arcs. In the design of a cycloid rotor profile with a small rolling circle, the rolling circle radius is less than 1/4 of the pitch circle radius, which yields a new cycloid rotor profile composed of an epicycloid, a hypocycloid, and arcs. The rotor profile was designed considering a Roots vacuum pump with a pumping speed of 70 L/s as an example. It was observed that, in the cycloid rotor profile with a large rolling circle, as the rolling circle radius increases, the volume utilization rate increases. When the ratio of the pitch radius to the rolling circle radius is less than 2, the volume utilization rate is 20% better than that of the standard cycloid profile and is also better than that of the arc and involute rotor profiles, which has evident advantages. In the cycloid rotor profile with a small rolling circle, as the rolling circle radius decreases, the volume utilization rate decreases; however, the length of the minimum gap between the rotor and the chamber increases, which can reduce the backflow and increase the compression ratio and ultimate vacuum. Certainly, the volume utilization rate and the length of minimum gap are not optimized simultaneous by the new cycloid profiles. Therefore, further research and exploration are necessary to improve both volume utilization rate and minimum gap length simultaneous.

Acknowledgements The research leading to these results received funding [Science and Technology Program of Gansu Province in China] under Grant Agreement No. [21ZD4GA004].

Author's contribution ZL: formal analysis, validation, writing, methodology, XW: conceptualization, investigation, software, funding acquisition.

Funding The research leading to these results received funding [Science and Technology Program of Gansu Province in China] under Grant Agreement No. [21ZD4GA004].

Declarations

Conflict of interest The authors declare that they have no known competing financial interests or personal ties that may have influence our work.

References

1. Vecchiato D, Demenego A, Argyris J et al (2001) Geometry of a cycloidal pump. Comput Appl Mech Eng 190:2309–2330
2. Hsieh C-F, Hwang Y-W (2007) Study on the high-sealing of Roots rotor with variable trochoid ratio. Math Comput Model 129(12):1278–1284
3. Wang S, Li H, Zhao Y (2011) The improvement study of involutes profile type rotor in Roots vacuum pump. In: 2011 International conference on new technology of agricultural engineering (ICAE 2011), Zibo, China
4. Hwang Y-W, Hsieh C-F (2006) Study on high volumetric efficiency of the Roots rotor profile with variable trochoid ratio. Mech Eng Sci 220:1375–1385
5. Yang DCH, Tong S-H (2002) The specific flowrate of deviation function based on lobe pumps derivation and analysis. Mech Mach Theory 37:1025–1042
6. Wang J, Liu R, Yang S et al (2018) Geometric study and simulation of an elliptical rotor profile for Roots vacuum pumps. Vacuum 153:168–175
7. Wu Y-R, Tran V-T (2018) Generation method for a novel Roots rotor profile to improve performance of dry multi-stage vacuum pump. Mech Mach Theory 128:475–491
8. Hsieh C-F, Hwang Y-W (2008) Tooth profile of a Roots rotors with a variable trochoid ratio. Math Comput Model 48(1–2):19–33
9. Jung S-Y, Han S-M, Cho H-Y et al (2009) Automated design system for a rotor with an ellipse lobe profile. J Mech Sci Technol 23:2928–2937
10. Kwon S-M, Kang HS, Shin J-H (2009) Rotor profile design in a hypogerotor pump. J Mech Sci Technol 23:3459–3470

11. Wu Y-R, Fong Z-H (2008) Rotor profile design for the twin-screw compressor based on the nomal-rank generation method. J Mech Des 130:042601
12. Hsieh CF, Zhou QJ (2015) Fluid analysis of cylindrical and screw type Roots vacuum pumps. Vacuum 121:274–282
13. Zhang S, Song A, Tian D, Tao J (2014) Design and simulation of the outline of Roots pump rotor. Mech Derive 38(3):91–93
14. Zhou S, Jia X, Yan H, Peng X (2021) A novel profile with high efficiency for hydrogen circulating Roots pumps used in FCVs. Int J Hydrogen Energy 46:22122–22133
15. Qin L, Liu Y (1990) Study on the profile of circular arc rotor of Roots pump. Vacuum 1:32–33